The African Review of Physics (2018) 13: 0005

Synthesis and Characterization of a dual-doped Zinc Oxide [(Na,N):ZnO] Nanoparticles by Wet Chemical Method

A. Habeebullah[1]*, A.B. Alabi[1], O.A. Babalola[1], E.D. Kajewole[1], T.J. Adeleke[1] and T. Akomolafe[1]
[1]*Department of Physics, University of Ilorin, Ilorin, Nigeria*
Email Address: drrammys@yahoo.com

Zinc Oxide (ZnO) nanoparticles have been prepared through the wet chemical route at a low temperature of 60^0C and dried at 80^0C for 5hrs using zinc acetate dehydrate as a starting material. The as-prepared powder was doped with dual acceptor (Na,N) at 5 and 10% molar concentration using Sodium Acetate and Ammonium Acetate as Na and N source, respectively. AAS, FTIR, XRD, UV-VIS Spectroscopy, and Hall measurement were used to study the metallic element present, chemical bonding, structural morphology, optical, and electrical properties of the nanoparticles, respectively. AAS revealed the presence of Zn and Na concentration within the standard range. The FTIR spectra observed at 480.28 cm^{-1} and 470.63 cm^{-1}confirmed the Zn–O bond stretching. XRD results showed the formation of ZnO nanoparticles having polycrystalline single-phase nature with hexagonal wurtzite crystal structure. The crystallite size has been found to vary between 18.1nm and 21.6 nm with changes in the doping concentration of (Na,N). High transparency in the visible region (above 90%), narrowing of direct optical bandgap (3.46-3.01eV) as dopants increase because of the s–d and p–d exchange interactions, which introduce a negative and a positive correction to the conduction and the valence-band edges respectively showed distinct optical features. The electrical characterization of the dual-doped (Na,N):ZnO exhibit p-type conductivity, with the lowest resistivity of 5.80×10^{-2} Ω-cm for the 10% molar concentration. These results make dual acceptor doped (Na,N):ZnO a promising material for application in photovoltaic solar cells and other optoelectronics devices.

1. Introduction

Nanomaterials are being widely investigated because of their fascinating optical, electronic and mechanical properties [1]. Semiconductor nanoparticles (NPs) in particular have been found to have large surface area to volume ratio, unique optical and electronic properties compared to those of their bulk counterpart [2]. ZnO is an II–VI compound semiconductor transparent oxide; with a relatively large direct band gap of ~3.37 eV at room temperature. It becomes an attractive candidate to replace the standard transparent conducting oxide called indium tin oxide (ITO) for being rare and expensive; especially if doped with impurities, as this improve the electrical, structural and optical features of ZnO.

ZnO is a naturally *n-type* degenerate semiconductor and the lack of *p-type* conductivity continues to impede the development as it suffers greatly from the doping asymmetry problem, in that it can be doped *n*-type rather easily, but *p*-type proved to be a formidable challenge, which from a practical point of view has not been conquered yet. In general, the doping problem arises from the fact that wide-gap semiconductors either have a low valence-band maximum or a high conduction-band minimum [3,4].

Known acceptors used in achieving *p-type* ZnO are *group IA* elements (Li, Na, K), *group IB* elements (Cu, Ag, Au), *group III elements* (B, Al, Ga, In), *group VA* elements (N, P, As, Sb), and Zn vacancies depending on the application to be achieved. Intrinsic *p*-doping via Zn-vacancies is not reliable, because it is difficult to control the needed small deviations from stoichiometry and stability of non-equilibrium point defects. Therefore, the main approach for achieving *p*-type ZnO is the substitution of some of the host matrix elements with acceptor impurities.

One possible approach is the introduction of a *group IA* element, such as Li, Na, and K on Zn sites. As predicted by the density functional theory (DFT) [5], Li, Na, and K form acceptor levels at 0.09, 0.17, and 0.32meV above the maximum of the valence band, respectively. However, doping with *group IA* elements suffers from their very high diffusivities as well as self-compensation by occupying interstitial positions where they act as donors [6]. For instance, doping with lithium creates semi-insulating ZnO [7] because of additional interstitial Li atoms acting as donors [8] compensating the acceptors.

Dual-doping techniques are the newly introduced method that may fabricate stable *p-type* ZnO and has attracted attention in recent years [9]. Different groups have reported N co-doped with Li and Al. This resulted in Li forming $Li_{Zn}-Li_i$, $Li_{Zn}-H$ complexes [10], disappearance of *p-type* conductivity over time [11] and instability charge carrier type at higher annealing temperature [12]. This might be as a result of acceptor elements chose (elements has different atomic radius and energy formation), higher post heat treatment (causes the solid phase reaction and diffusion between the materials) and inability to control the material composition and stoichiometry (method of synthesis adopted). Homo-junction light-emitting diodes utilizing *p*-type ZnO doped with Na have also been reported recently [13]. P-type layers showed hole concentration varying from $4.85x10^{17}$ cm^{-3} to $4.7x10^{18}$ cm^{-3} with low Hall mobility ranging from

0.12 to 1.42 cm^2/Vs. Also, the ionization energy of Na acceptor was found to be 0.164 eV in agreement with the theoretical value of 0.17 eV [8].

A wide range of synthetic methods are currently available for developing different morphologies of ZnO nanostructures, which result in a variety of material applications. These include hydrothermal [14], sol–gel organometallic [15], pyrolysis [16], laser ablation, and vapour phase epitaxial growth [17] with each method unique and their result most often differs depending on the experimental parameters.

We, therefore, reported *p-type* dual-doped acceptor (Na,N):ZnO by wet chemical method since research on the combination of this two acceptor elements is rare. Also, the method used is simple, cost effective and offers an extremely easy way for preparing nanoparticles of desired composition and stoichiometry.

2. Experimental Details

2.1 Synthesis

The precursor was prepared by adding 25ml of distilled water to 0.65g of Zinc Acetate Dehydrate at room temperature, (Sodium Acetate, Ammonium Acetate as sodium and nitrogen source was added to the starting solution of Zinc Acetate Dehydrate with the atomic ratio of Na and N being 6:2. This procedure was repeated for 5%, and 10% dopant concentration for the dual doped sample. 1.83 ml of Ammonium hydroxide was then added in drop with continuous stirring for 15 minutes using a magnetic stirrer until a homogeneous and stable colloid solution was formed. Thereafter, 11.65 ml of sodium hydroxide was added to the homogenous solution forming transparent white solutions and stirred for 1 hour at room temperature.

The overall solution was heated at 60^0C for 3 hours in an oven and rinsed with distilled water and ethanol, then filtered (as ethanol can react more easily to form a polymer precursor with a higher polymerization degree of hydroxyl complex to form "Zn–O–Zn" bridges). The precipitate residues obtained were dried at 80^0C for 5 hours in a furnace.

2.2 Characterization Techniques

The concentration of the metallic elements present in the nanoparticles synthesized was determined using Atomic Absorption Spectrophotometer AAS (Model: BUCK Scientific ACCUSYS 211) and Flame Photometer (Model: Sherwood 410). The chemical bonding and spectra features was analysed by Fourier Transform Infrared (Spectrum 65, Shimadzu) in the range of 4000–400 cm^{-1} with a resolution of $1cm^{-1}$.The structural characteristics were studied by P'analytical System X-ray Diffractometer XRD (Model: DY-1656) using CuKα radiation (λ= 1.5406 Å) over a 2θ range of 20°–80°.The electrical resistivity was obtained using the van der Pauw four-point probe technique (KEITHLEY 2400), while carrier concentration, carrier type and mobility were obtained by Ecopia Hall Measurement System (HMS-5000) at a constant magnetic field strength 0.42T. The UV-Vis optical spectra were obtained with the help of automated spectrophotometer (Shimadzu, UV-6800) in the wavelength range of 200 to 620 nm.

3. Results and Discussion

3.1 Elemental Characterization

The qualitative and quantitative determination of the metallic elements present in the un-doped and doped nanoparticles was characterized by Atomic Absorption Spectrophotometer and Flame Photometer. The table below showed the standard and observed characteristic concentration of the synthesized dual- doped (Na,N):ZnO nanoparticles.

Table 1. Standard and Sample Concentration

Elements	Standard Concentration (mg/L)	Synthesized Sample Concentration (mg/L)	
		Un-doped	Dual-Doped
Zinc (Zn)	0.5 – 1.5	0.92	1.01
Sodium (Na)	1.2 – 2.5	------	2.3

characteristics of Dual-Doped ZnO

According to the obtained result, both the un-doped and dual-doped ZnO concentration falls within the standard range, revealing the uniqueness of the wet chemical synthesis. Moreover, addition of impurities resulted in an increment of the ZnO concentration, which can be attributed to the increase in ZnO growth.

3.2 Functional Characterization

The determination of the chemical bonding in the prepared nanoparticles was studied using Fourier Transform Infrared.

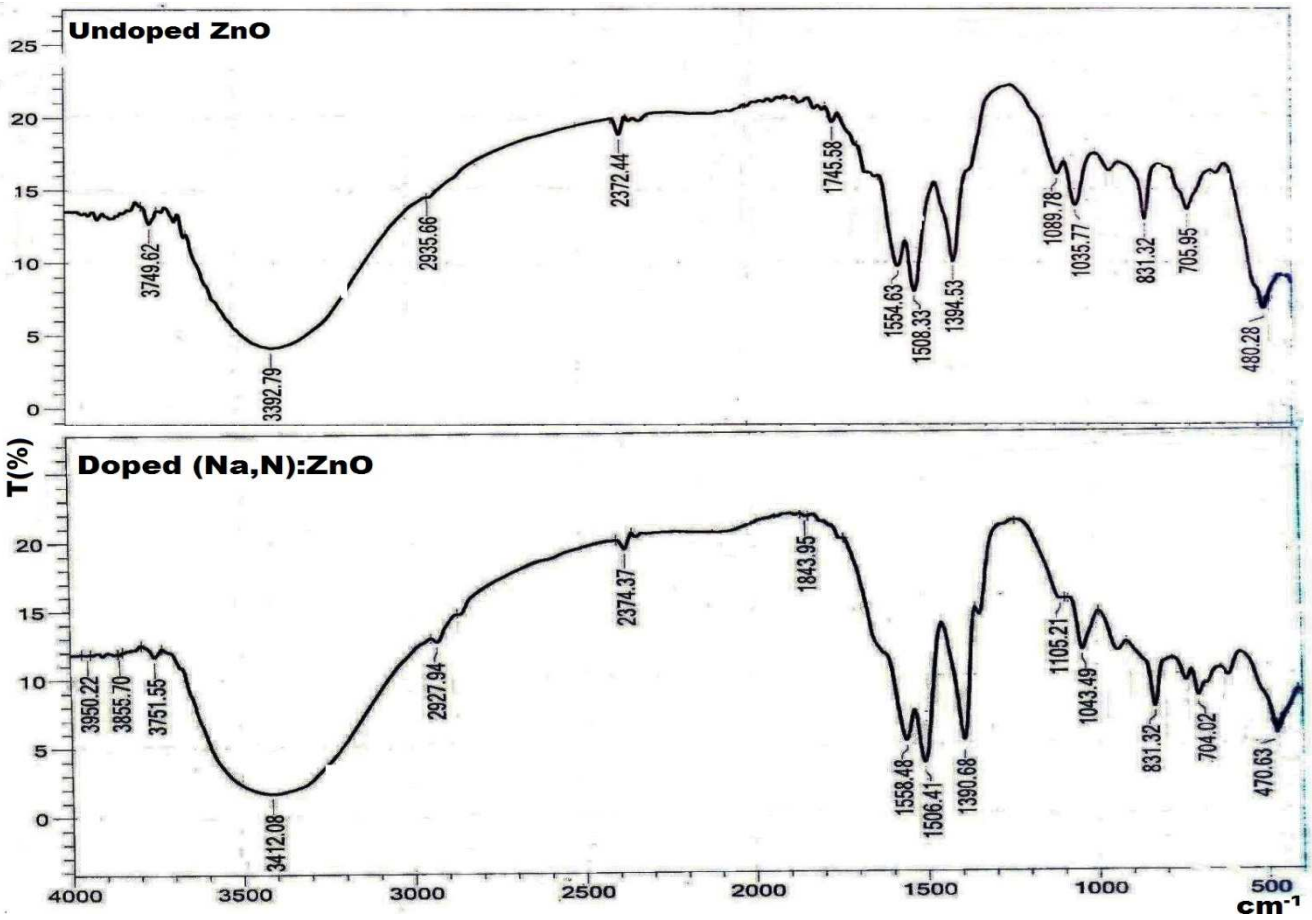

Fig. 1. FTIR absorption spectra of Un-doped and dual-doped ZnO Nanoparticles

The Infrared modes 380-750cm^{-1} corresponds to Zn–O bond in prepared nanoparticles; with the strongest around 380-550cm^{-1} [18]. Therefore, the absorption spectra band observed at 480.28 and 470.63 cm^{-1} for the un-doped and dual-doped sample can be attributed to the ZnO stretching vibration [19]. The vibrational mode at 831.32cm^{-1}common to the both sample due to substitutional hydrogen at oxygen site (H_O) bound to the lattice Zn site (i.e., Zn–H_O). This substitutional hydrogen may act as a shallow donor in ZnO [20].

The modes around 1000–1550 cm^{-1} were observed for both samples and these modes were usually assigned to O–C=O (symmetric and asymmetric stretching) vibrations due to ambient environment [21]. The band at 1745.58cm^{-1} and 1843.95cm^{1} observed in the un-doped and dual-doped ZnO was a characteristic of (COO–Zn) stretching due to partial decomposition of Zinc Acetate Dehydrate during the synthesis [22]. C–H local vibrational modes between 2800 and 3100 cm^{-1} have been observed in a number of semiconductor such as amorphous silicon carbon (a-SiC:H), GaAs, and GaN [23].

In these materials the local vibrational modes of 2935.66 and 2927.94cm^{-1} were assigned to C–H stretching modes.

The broad absorption spectra band at 3392.79-3749.62cm^{-1} for un-doped sample and 3412.08-3950.22cm^{-1} for dual-doped sample were attributed to the O–H stretch of the hydroxyl vibration due to the presence of hydrated H_2O molecules. Hence indicates more hydration of the dual-doped samples with additional peaks.

3.3 Structural Characterization

Fig. 2. showed the X-ray Diffraction pattern of dual acceptor doped (Na,N):ZnO. The XRD pattern was obtained in 2θ range of 20–80°, with Cu Kα radiation source (λ=1.5402 Å) to determine their crystal structure and phase orientation.

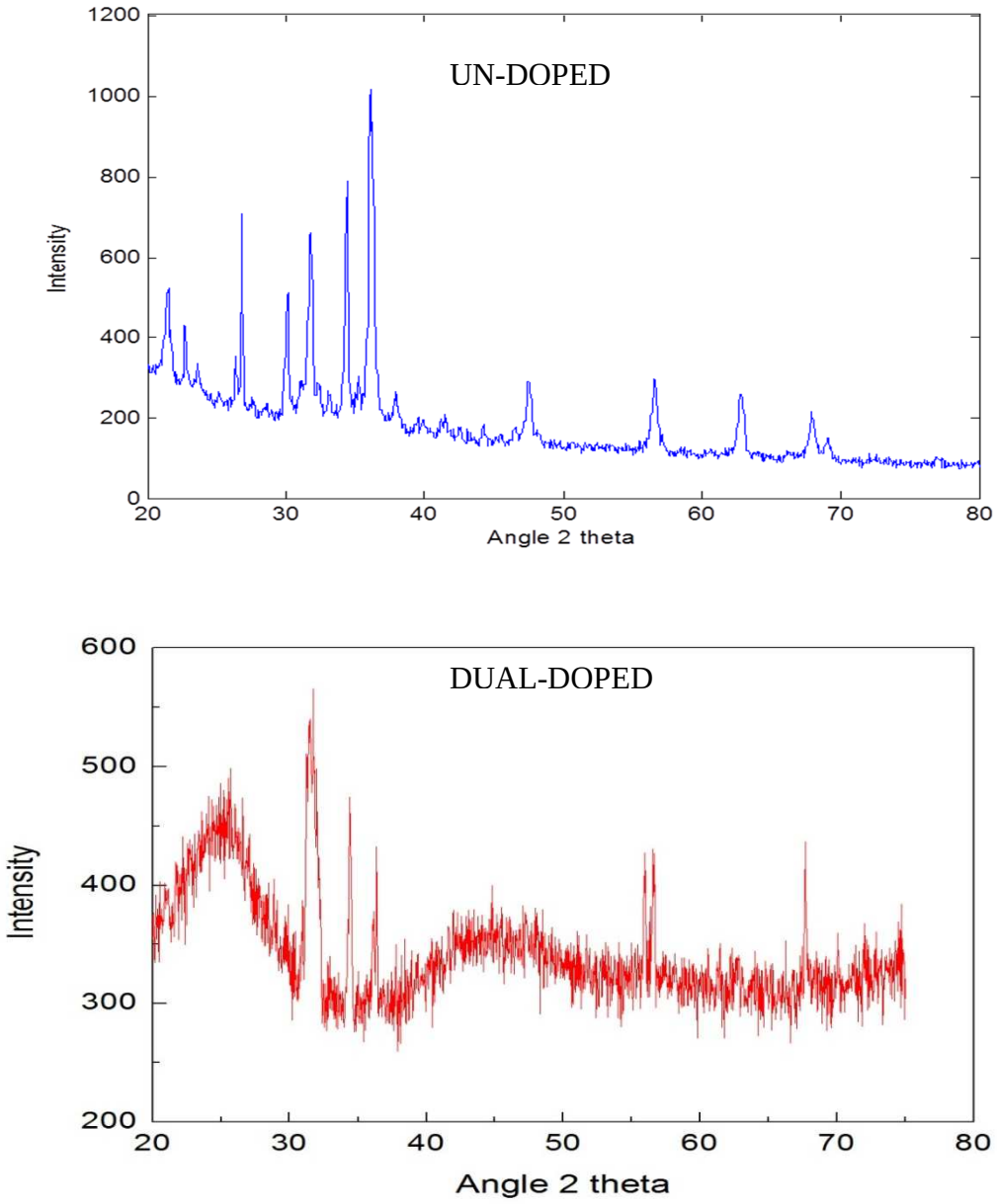

Fig. 2. XRD pattern of un-doped and dual-doped ZnO Nanoparticle

The diffraction peaks in Fig. 2 located at 31.75˚, 34.56˚,36.23˚,47.59˚, 56.58˚, and 67.69˚ corresponding to crystal orientation (100), (002), (101), (102), (110), and (201) matched (JCPDS card 79-0205), and have been keenly indexed as hexagonal wurtzite phase of ZnO. The absence of secondary phases indicates that dopants did not alter the wurtzite structure of ZnO.

The dual doped ZnO revealed unobvious XRD patterns of ZnO as a result of impurities, suggesting that the dual-doping with Na and N strongly affects the crystallization of ZnO leading to higher degree of amorphousity of ZnO. This makes Zinc Oxide a prospective candidate for transparent amorphous oxides.

Usually, ZnO prefer to grow in (002) orientation due to low surface energy of formation. Un-doped ZnO had the strongest reflection at (101) plane, which was the densest plane of this sample showing after growth orientation. On the other hand, dual-doped had the strongest reflection at (100), the densest plane of this sample showing an initial growth. Recent reports on nitrogen doped ZnO revealed the presence of the (100) crystal orientation related to the presence of nitrogen on the Zinc Oxide compound [24].

The crystallite size D was calculated from the Debye-Scherer formula.

$$D_{avg.} = \frac{k\lambda}{\beta \cos\theta}(nm) \qquad (1)$$

Where: $\lambda, \beta, k, \theta$ are X-ray wavelength (1.5402 Å), full width at half maximum of the diffraction peak, Debye Scherrer Constant (0.94), and the diffraction angle, respectively.

The average crystallite size of un-doped and dual-doped ZnO was 18.1 nm and 21.6 nm respectively. This confirms nanoscale size of the synthesized ZnO and the incorporation of (Na,N) ions on Zn and O substitutional or interstitial sites which improve the stoichiometry and solubility of dual doped ZnO.

As shown in Table 1, The Inter-planar spacing (d_{hkl}), was calculated using the Bragg's relation.

$$n\lambda = 2d\sin\theta \qquad (2)$$

The *d* spacing value was high in dual-doped sample compared to un-doped. This could be as a result of the difference in ionic radius between Na^+ (102 pm) and Zn^{2+} (74pm), N (171nm) and O (140nm). Higher ionic radius replaced lower ionic radius at their site, redistribute the atom and contribute to inter planar spacing [25]. Hence, the replacement of larger ion on smaller ionic site increases the *d* spacing.

The dislocation or defect density was calculated by the formula:

$$\delta = \frac{1}{D^2}(nm^{-2}) \qquad (3)$$

The value for un-doped and dual-doped ZnO were $3.05 \times 10^{-3} nm^{-2}$ and $4.57 \times 10^{-3} nm^{-2}$, respectively. This confirmed that the un-doped ZnO is purer with lesser defects because the lower the dislocation density the better is the quality of the crystallized powder [26].

However, the presence of local lattice disorders may lead to obvious reduction in intensities of XRD peaks (Fig. 1) attributed to destroyed periodicities in crystal planes.

The residual stress for the as-prepared (Na,N):ZnO were calculated using the formula:

$$\sigma = -233\frac{c - c_0}{c_0}(GPa) \qquad (4)$$

Where c_0 is (5.2066Å) - the unstrained ZnO lattice constant.

The value was 0.0448 GPa and −0.0850 GPa for both un-doped and dual-doped sample, respectively. The negative sign indicates that the residual stress in the dual-doped ZnO was compressive with elongated lattice constant [27]. The decrease in the residual stress with dual doping may be attributed to the decrease in diffusion and the rate of reaction between the free zinc and oxygen due to Na, N incorporation, which led to an increase in their concentration (as confirmed from the AAS result), thereby create a tension in the lattice constant during the growth process.

The Lattice Constant was also evaluated using the formula:

$$a = b = \frac{\lambda}{\sqrt{3}\sin\theta}; c = \frac{\lambda}{\sin\theta}(\text{Å}^o) \qquad (5)$$

The values of *a* and *c* were 3.2479Å and 5.2056Å; 3.2528Å and 5.2085Å for un-doped and dual-doped, respectively. The standard values of *a* and *c* for the hexagonal structure of ZnO were 3.253Å and 5.265Å. Hence, these standard values were very close to our reported values.

Parameters / Samples	Avg. Crystallite Size D (nm)	Inter-planar Spacing d_{hkl}(Å)		Defect Density □(nm^{-2})	Residual Stress: σ(GPa)	Lattice Constants (Å)	
		d_{100}	d_{002}			**A**	**c**
Un-doped ZnO	18.1	2.8127	2.6028	3.05×10^{-3}	0.0448	3.2479	5.2056
Dual Doped ZnO	21.6	2.8162	2.6043	4.57×10^{-3}	-0.0850	3.2528	5.2085

Table 2. Crystal Structural Parameters of Un-doped and dual-doped ZnO

3.4 Electrical Characterization

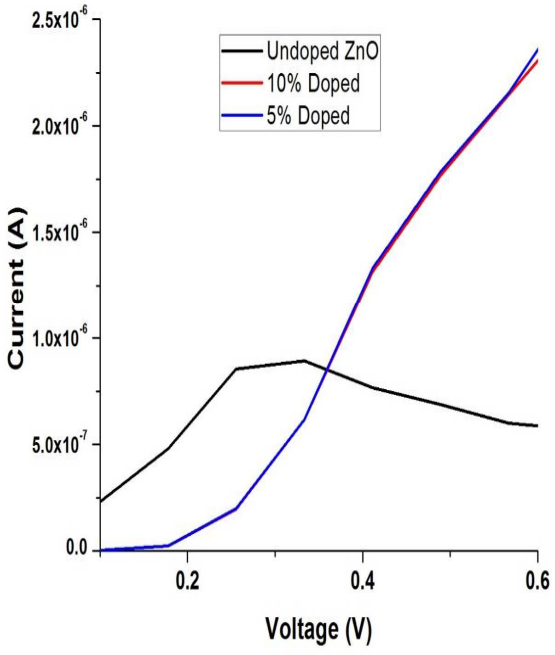

Fig. 3. Typical I-V characteristics of synthesized Un-doped and Dual-Doped ZnO Nanoparticles.

The electrical properties of dual-doped (Na,N):ZnO NPs were shown in the graph as measured using 4-Point Probe technique to understand the (I-V) characteristics.

The non-linear curve for both sample as shown in Fig.3. confirmed the synthesized sample is a semiconductor being non-ohmic. The current increases as more dopants were introduced.

Also, the graph showed the resistance of 10% dual doped ZnO was the lowest. This was due to the free electron that will be generated with low resistance. The substitution of Na with Zn and N with O produces free electron that increase the carrier concentration in nanoparticles.

The nature (*p or n-type*) of conduction in the (Na,N):ZnO NPs was also determined in Table 2 below based on Hall measurement. Prior the measurement, samples were cut in $0.5\times1.5cm^2$ and silver metal ohmic contacts performed and tested.

According to table 3.4, the un-doped ZnO nanoparticles showed *n-type* conductivity, highest resistivity of $3.296\times10^3\Omega cm$ with lowest carrier concentration of $5.67\times10^{15}cm^{-3}$. The source of this conductivity is due to intrinsic defects such as oxygen vacancies (V_O) [28, 29], acting as deep donors, interstitial Zn (Zn_I) [30] and Zn anti-sites (Zn_O^{2+}) forming shallow donor levels [29], and background hydrogen acting as donor at interstitial sites [31].

The dual-doped ZnO showed *p-type* conductivity, increase in carrier concentration (~10^{17} to 10^{18} cm^{-3}), with 10% (Na,N):ZnO having the lowest resistivity (0.058 Ωcm).The decrease in electrical resistivity in as-grown dual doped NPs can be interpreted mainly by the increase in free carrier concentration provided by Na and N ions acting as (Na_{Zn}-N_O) acceptor complex

formation when incorporated in substitutional or interstitial positions [32]. Another reason was due to the improvement of crystal quality and the consequent increment in mobility, as mobility is enhanced by the increase in grain size (reported in the structural characterization). The increase in carrier concentration could be attributed to the ionization of oxygen vacancies (Vo) followed by oxygen annihilation from the ZnO crystals and by desorption of oxygen in the grain boundaries which acts as traps for the carriers [33].

Table 3. Electrical properties of as grown Na-N dual acceptor doped ZnO NPs

Samples	Resistivity (Ω cm)	Conductivity $(\Omega\ cm)^{-1}$	Hall Coefficient (cm^3/C)	Charge Density (Ccm^{-3})	Mobility $(cm^2V^{-1}s^{-1})$	Carrier concentration (cm^{-3})	Carrier type
Undoped	3.296×10^{3}	3.033×10^{-4}	1101.20	9.081×10^{-4}	0.334	5.67×10^{15}	*n*
5% Doped	0.144	6.944	7.692	1.3×10^{-1}	53.4	8.125×10^{17}	*p*
10% Doped	0.058	17.241	2.071	4.829×10^{-1}	35.7	3.018×10^{18}	*p*

3.5 Optical Characterization

The optical properties of Na-N dual-doped ZnO nanoparticles were investigated using UV-VIS Spectrophotometer in the wavelength range 200-620 nm.

3.5.1 Absorption Analysis

The absorption spectrum of ZnO nano-powder is shown in Figure 3.5.1. The absorption peak at about 248nm due to the ZnO nanoparticles lies much below the band gap wavelength of bulk ZnO (388nm) and hence indicates monodispersed nature of the nanoparticle distribution [34]. The result was in accordance with the bandgap value of the bulk ZnO (3.37 eV) in which ZnO absorbs only a small portion of ultraviolet (UV) range.

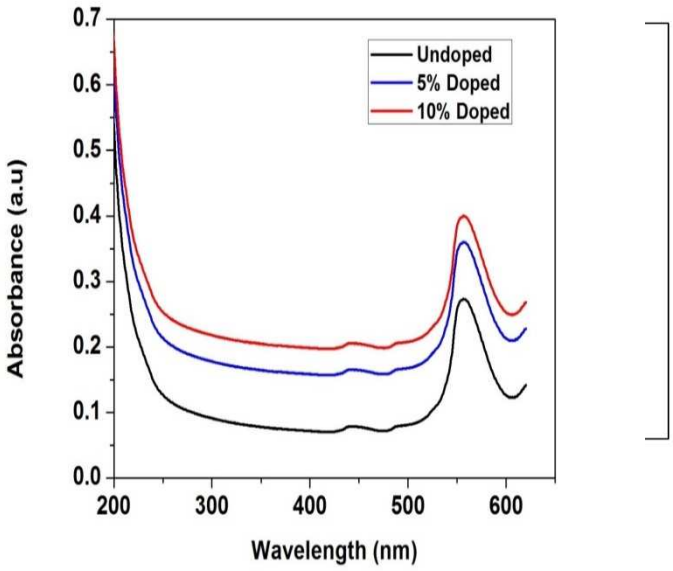

Fig. 4a. Absorption spectra of the Un-doped and Dual-Doped ZnO Nanoparticles
Fig. 5b. Energy Bandgap of the Un-doped and Dual-Doped ZnO Nanoparticles

The optical bandgap (E_g) has been determined from the plots of $(\alpha h\nu)^2$ vs. photon energy ($h\nu$) for un-doped and dual-doped ZnO, respectively. The direct band gap energy was obtained from intercept on the energy

axis after extrapolation of the straight line section of $(\alpha h\nu)^2$ vs. hν curve calculated using Tauc's relation, given by:

$$\alpha h\nu = A(h\nu - E_g)^n \quad (6)$$

Where α is the absorption coefficient, $h\upsilon$ is the photon energy, A is the constant, E_g is the bandgap of the sample. The value of n is ½ for ZnO (direct band structure).

It has been found that, the values of band gap decreases with increasing (Na,N) dual-doped concentration. The bandgap of the un-doped ZnO was 3.46eV, while the dual-doped sample decreases as dopants increases from 5% to 10% (3.38-3.01eV). The band gap was narrowed because of the s–d and p–d exchange interactions which introduce negative and positive correction to the conduction and the valence-band edges, respectively [35].

3.5.2 Transmission Analysis

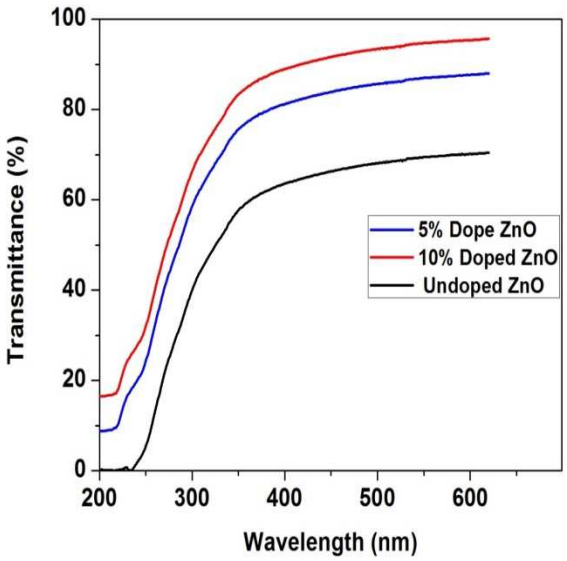

Fig. 5. Transmission spectra of the Un-doped and Dual Doped ZnO Nanoparticles

Fig. 5 showed the optical transmission spectra of as-prepared dual doped ZnO. Un-doped, 5% and 10% sample were in the wavelength range of 200-620nm. There was a prominent transmission edge in the visible range (400-620nm), suggesting good quality of ZnO attained by wet chemical technique.

Dual doped ZnO displayed significant enhanced transmittance in the visible region of 400-620 nm with more than 90% transparency. This was as a result of less absorption owing to optical interference effects making the possible to be used as window layers in photovoltaic solar cells.

4.0 Conclusion

Owing to cost efficiency and simplicity, wet chemical route proved to be a good technique for the preparation of dual acceptor doped (Na,N):ZnO nanoparticles. The effect of varying dopant's concentration on the properties of ZnO resulted in the presence of a reasonably high conductive *p-type* nanoparticles ($17.241(\Omega\ cm)^{-1}$) with carrier concentrations above $10^{18}cm^{-3}$. This improvement was associated to changes in the crystal orientation from (002) to (100) and (101), related to (Na,N) incorporation that also led to changes in the surface morphology and increase in crystallite size (from 18.1-21.6nm).

The high transmittance in the visible range (above 90%) and decrease of the direct narrowing optical bandgap (3.46-3.01eV) with increasing dopants concentration makes dual acceptor doped (Na,N):ZnO a promising material for application in photovoltaic solar cells and other optoelectronics devices.

Acknowledgements

The authors express their sincere gratitude to Mr. Rasheed, Dept. of Material Science, Kwara State University, Ilorin, for the characterization facilities provided.

References

[1] Bangale S.V., Prashale R.D., Bamane S.R.., (2011): "Effects of zinc nitrate, zinc acetate and zinc chloride on the properties of ZnO by chemical method"; *Journal of Chemical Pharmaceutical Resources.* Volume 6, page 527.

[2] Mohd. Arshad, Mohd. Meenhaz Ansari and Arham S. Ahmed (2015): "Band gap engineering and enhanced photoluminescence of Mg doped ZnO nanoparticles synthesized by wet chemical route"; *Journal of Luminescence*. Volume 161, page 275.

[3] Zhang S. B., Wei S.-H., and Zunger A., (1998): "A phenomenological model for systematization and prediction of doping limits in II-VI and I-III-VI2 compounds"; *Journal Applied Physics.* Volume 83, page**.**

[4] Zhang S. B., Wei S. -H., and Zunger A., (1999): "Overcoming doping bottlenecks in

semiconductors and wide-gap materials"; *Physical Bull.* Volume 273, page 976.

[5] Park C.H., Zhang S.B., and Wei S.H., (2002) "Origin of p-type doping difficulty in ZnO: The impurity perspective", *Physics Review Bull*. Volume 66, page073202.

[6] Look D.C. and Claflin B., (2004): "High-quality, melt-grown ZnO single crystals*"; Physical Status Solidi B.* Volume 241, page 624.

[7] Wardle M.G., Goss J. P., and Briddon P. R., (2005): "Theory of Li in ZnO: A limitation for Li-based p-type doping"; *Physical Review B*, Volume 71, page 155205.

[8] Park C.H., pg S.B., Su-Huai Wei, (2002): "Compensation mechanism for N acceptors in ZnO"; *Physical Review*. Volume 66, page 073202.

[9] Krtschil, A., Dadgar, A., Oleynik, N., Blasing, J., Diez, A., Krost, A., (2005): "Local p-type Conductivity in Zinc Oxide Dual-Doped with Nitrogen and Arsenic"; *Applied Physics Letters.* Volume 87, page 262105.

[10] Cox, R.T., Block, D., Herve, A., Picard, R., Santier, C., Helbig, R, (1978): "Exchange broadened, optically detected ESR spectra for luminescent donor-acceptor pairs in Li doped ZnO"; *Solid State Communications.* Volume 25, page 77.

[11] Barnes, T.M., Olson, K., Wolden, C.A., (2005): "On the formation and stability of p-type conductivity in nitrogen doped zinc oxide";*Applied Physics Letters*. Volume 86, page 421.

[12] Swapna R., Venkateswarlu K., Santhosh Kumar M. (2015): "Heat Treatment Impact on the Properties of Na and N Dual Doped ZnO Thin Films by Spray Pyrolysis"; *Procedia Materials Science.* Volume 10, Page 714.

[13] Lin S.S., Lu J.G., Ye Z.Z., He H.P., Gu X.Q., Chen L. X., Huang J.Y., and Zhao B.H., (2008): "Na doping concentration tuned conductivity of ZnO films via pulsed laser deposition and electroluminescence from ZnO homojunction on silicon substrate"; *Journal of Physical D*. Volume 41, page155114.

[14 Djuriˇsic´ A.B, Chen X, and Leung Y.H, Ng AMC (2012): "ZnO nanostructures: growth, properties and applications"; *Journal of Material Chemistry*. Volume 22, page 6526.

[15] Ismail R.A, Ali A.K, and Ismail M.M, Hassoon K.I (2011): "Preparation and characterization of colloidal ZnO nanoparticles using nanosecond laser ablation in water"; *Journal of Applied Nanoscience.* Volume 1, page 45.

[16] Samanta P.K, Bandyopadhyay A.K (2012): "Chemical growth of hexagonal zinc oxide nanorods and their optical properties"; *Journal of Applied Nanoscience.* Volume 2, page 111.

[17] Zhan X, Chen F, Salcic Z (2012): "Synthesis of ZnO submicron spheres by a two-stage solution method"; *Applied Nanoscience*. Volume 2, page 63.

[18] Wahab, Rizwan, S.G. Ansari, Young Soon Kim, Minwu Song, and Hyung-Shik Shin, (2009): "The role of pH variation on the growth of zinc oxide nanostructures"; *Applied Surface Science.* Volume 255, page 4891.

[19] Ivanova T; Harizanova A; Koutzarova T; and Vertruyen B; (2010): "Study of ZnO Sol-Gel films, effect of annealing"; *Materials Letters*. Volume 64, page 1147.

[20] Senthil kumar K., Tokunaga M., Okamoto H., Senthil kumar O., Fujita Y., (2010): "wet chemical synthesis of ZnO NPs"; *Applied Physics Letter.* Volume 97, Page 091907.

[21] Renu Kumari, Anshuman Sahai, Navendu Goswami, (2015): "Effect of nitrogen doping on structural and optical properties of ZnO nanoparticles"; *Progress in Natural Science Materials International*. Volume 25, page 300.

[22] Wallace R; Brown A.P; Brydson R; Wenger K; and Milne S.J; (2013): "Synthesis of ZnO nanoparticles by flame Chemical Spray Pyrolysis and Characterization Protocol"; *Journal of Materials Science*. Volume 48, page 6393.

[23] Saleh R., Munisa M. and Beyer W., (2003): "Infrared Absorption in a-SiC:H Films Prepared by DC Sputtering"; *Thin Solid Films.* Volume 426, page 117.

[24] Golshahi S.M. Rozati, Martins R., Fortunato E., (2009): "*P-type* ZnO thin film deposited by spray pyrolysis technique, the effect of solution concentration"; *Thin Solid Films*. Volume 518, page 1149.

[25] Zi-qiang, X., Hong, D., Yan, L. & Hang. C. (2006): "Al-doping effects on structure, electrical and optical properties of c-axis-orientated ZnO-Al thin films"; *Materials Science in Semiconductor Processing.* Volume 9, page 132.

[26] Abdel-Sattar Gadallah and M.M. El-Nahass (2013): "Structural, Optical Constants and Photoluminescence of ZnO Thin Films Grown by Sol-Gel Spin Coating"; *Advances in Condensed Matter Physics.* Volume 10, page 1155.

[27] Reeber, R. R. (1970): "Lattice parameters of ZnO from 4.2° to 296° K. J."; *Applied Physics*. Volume 41, page 5063.

[28] Walukiewicz W., (1999): "Defect formation and diffusion in heavily doped semiconductors"; *Physics Review Bulletin.* Volume 50, page 5221.
[29] Janotti A. and Van de Walle C.G., (2005): "Oxygen vacancies in ZnO"; *Applied Physics Letter*. Volume87, page 122102.
[30] Look D. C., Hemsky J. W., and Sizelove J. R., (1999): "Residual Native Shallow Donor in ZnO"; *Physics Review Letter.* Volume 82, page 2552.
[31] Van de Walle C.G., (2000): "Hydrogen as a Cause of Doping in Zinc Oxide"; *Physics Review Letter.* Volume 85, page 1012.
[32] El Manouni A., Majon F.J., Mollar M., Mari B., Gomez R., Lopez M.C., Ramos-Barrado J.R., (2006): *Super-lattices Microstructure.* Volume 39, page 185.
[33] Major S., Banerjee A., Chopra K.L., (1984): "Annealing studies of un-doped and indium-doped zinc oxide"; *Thin Solid Films.* Volume 122, page 31.
[34] Zhang D. H., XueZ. Y., and Wang Q. P., (2002): "Formation of ZnO nanoparticles by the reaction of zinc metal with aliphatic alcohols"; *Journal of Physics D*. Volume 35, page 2837.
[35] Singh P., Koushal A., and Kaur D., (2009): "Mn-doped ZnO Nanocrystalline Thin Films Prepared by Ultrasonic Spray Pyrolysis"; *Journal of Alloy Compound*. Volume 471, page 11.

Received: 17 December, 2016
Accepted: 20 April, 2018